Journal Pre-proof

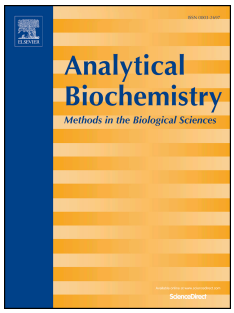

A Novel Fluorescent Probe with Extremely Low Background Fluorescence for Sensing Hypochlorite in Zebrafish

Zhixiang Han, Lianghuan Dong, Fan Sun, Lingliang Long, Shu Jiang, Xiaoting Dai, Min Zhang

PII: S0003-2697(20)30327-4

DOI: https://doi.org/10.1016/j.ab.2020.113795

Reference: YABIO 113795

To appear in: *Analytical Biochemistry*

Received Date: 16 February 2020

Revised Date: 4 May 2020

Accepted Date: 20 May 2020

Please cite this article as: Z. Han, L. Dong, F. Sun, L. Long, S. Jiang, X. Dai, M. Zhang, A Novel Fluorescent Probe with Extremely Low Background Fluorescence for Sensing Hypochlorite in Zebrafish, *Analytical Biochemistry*, https://doi.org/10.1016/j.ab.2020.113795.

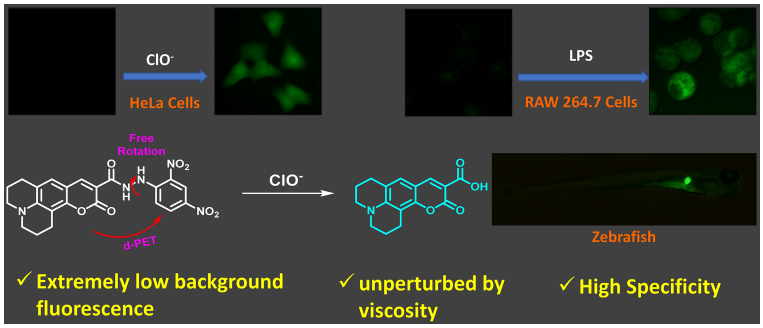

A Novel Fluorescent Probe with Extremely Low Background Fluorescence for Sensing Hypochlorite in Zebrafish

Zhixiang Han,*[,a] Lianghuan Dong, [a] Fan Sun,[a] Lingliang Long,*[,b] Shu Jiang,[a] Xiaoting Dai,[a] and Min Zhang[b]

[a]School of the Environment and Safety Engineering, Jiangsu University, Zhenjiang, Jiangsu 212013 (P. R. China).

[b]School of Chemistry and Chemical Engineering, Jiangsu University, Zhenjiang, Jiangsu 212013 (P. R. China).

* Corresponding author:

Fax: +86-511-88790955

Email: zhixianghan69@126.com; longlingliang@ujs.edu.cn.

Abstract

Development of an efficient fluorescent probe for sensing hypochlorite in water samples and biological samples is highly demanded. However, the currently reported fluorescent probes for hypochlorite frequently suffered from the problem of high background fluorescence. Herein, based on the combined effect of two different fluorescence quenching groups, we rationally developed a novel fluorescent probe for hypochlorite with extremely low background fluorescence. Notably, due to the doubly quenching groups, the probe could even keep low background fluorescence in a solution with high viscosity. Furthermore, the probe displayed highly sensitive and selective response to hypochlorite, with the detection limits calculated to be 10.5 nM. Practical application

demonstrated that the probe was able to quantitatively detect hypochlorite in various water samples with good recovery. Significantly, the probe showed extremely low background fluorescence in living cells and was capable of detecting minor variation of endogenous hypochlorite in RAW 264.7 cells. Moreover, the fluorescence imaging different concentration of hypochlorite in zebrafish has been successfully conducted. The probe developed herein will be widely used as a reliable tool to accurately monitor the variation of hypochlorite in living organism.

Keywords: Fluorescent probes, Doubly-quenching groups, Low background detection, Hypochlorite, Zebrafish.

1. Introduction

Hypochlorite (ClO^-), a common reactive oxygen species (ROS), has been extensively used in our daily lives as disinfectant and household bleaching agent [1]. Generally, it is used in a concentration range of 10 -10^4 μM. Nevertheless, exposure to high levels of ClO^- residue in water may cause eye/nose irritation and stomach discomfort, and thus pose severe adverse effect to human health. On the other hand, ClO^- can be endogenously produced in living organism by the reaction of H_2O_2 and Cl^- under the catalysis of myeloperoxidase (MPO). It plays significant roles in human immune system and maintaining intracellular redox homeostasis. However, imbalance of ClO^- concentration in human body often causes oxidative stress related diseases, such as cardiovascular diseases [2], lung injury [3], rheumatoid arthritis [4], and other diseases [5]. Therefore, construction of an efficient method for detection of ClO^- in water samples and biological samples is urgently required.

Recently, several strategies for detection of ClO^- have been developed, including

spectrophotometry [6], colorimetric assays [7], chemiluminescence method [8], electrochemical analysis [9], fluorescent probe, and so on. Compared with other strategies, the fluorescent probe has gained especially attention due to its superior properties of high selectivity and sensitivity, facile operation, and capability for detecting analyte of interest in biological system in non-invasive way. So far, many fluorescent probes have been devised for detection of ClO^- based on its strong oxidation reactivity to acylhydrazines [10], chalcogenides [11-13], hydrazones [14], oximes [15], *p*-methoxyphenols [16], ether [17], and C=C bonds [18]. However, despite the fabulous developments, the currently reported fluorescent probes often suffered from the problem of high background fluorescence from the probes themselves. For practical application, the residual background fluorescence signal tends to decrease the detection sensitivity, and even cause false positive results. To get an accurate and reliable detection, the fluorescent probe for ClO^- with extremely low background fluorescence is highly desirable.

In our previous work, we developed compound **1b** as fluorescent probe for ClO^- (Scheme 1) [19]. For probe **1b**, the free rotating N-N group was considered to be fluorescence quenching group for 7-diethylamino-coumarin fluorophore. Upon treatment with ClO^-, the N-N group can be selectively removed and thus the fluorescence of 7-diethylamino-coumarin fluorophore was recovered. It is known that the free rotation of a specific group was tightly associated with viscosity of surrounding medium [20]. The free rotation of N-N bond in **1b** might be significantly inhibited in a solution with high viscosity. Therefore, probe **1b** possibly exhibits high background fluorescence in living cells, as the viscosity is varied in distinct regions of the living cells [21].

Herein, on the basis of compound **1b**, we would like to design compound **LH-1** as a novel fluorescent probe for ClO^- with extremely low background fluorescence (Scheme 1). In compound **LH-1**, the coumarin 6H (blue color) was used as fluorophore. Compared with 7-diethylamino-coumarin (red color in **1b**), the coumarin 6H with twist-blocked and stronger electron-donating julolidine group exhibits higher quantum yield, better biocompatibility, as well as less background fluorescence when suppressed by a fluorescence quenching group [22-23]. Thus, the coumarin 6H in probe **LH-1** may help to reduce the background fluorescence. Importantly, apart from the free rotating N-N group as fluorescence quenching strategy, the 2,4-dinitrobenzene group in **LH-1** can be used as the second type of fluorescence quenching group, owing to the 2,4-dinitrobenzene group frequently resulted in fluorescence quenching of a fluorophore via donor-excited photoinduced electron transfer (d-PET) mechanism [24]. Consequently, probe **LH-1** was expected to exhibit extremely low background fluorescence by the combined effect of two different types of fluorescence quenching groups. In addition, as the d-PET based fluorescence quenching group will not be influenced by medium viscosity, probe **LH-1** would even display low background fluorescence in a solution with high viscosity, which is favourable for the probe applying in complex biological environment.

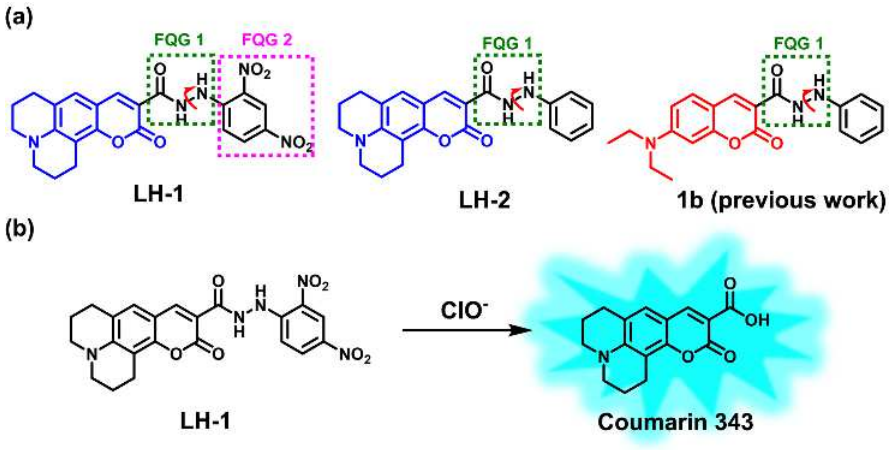

Scheme 1. (a) The molecular structures of compound **LH-1**, **LH-2**, and **1b**. The FQG represents fluorescence quenching group. (b) The sensing reaction of **LH-1** with ClO^-.

2. Experimental

2.1. *Materials and instruments*

Unless otherwise noted, all the chemical and biological reagents were purchased from commercialized companies and used without further purification. 8-hydroxyjulolidine-9-aldehyde (compound 4) was synthesized according to the literature procedure [25]. Twice-distilled water was prepared by UPU ultrapure water machine UPC-1-5, was used throughout all experiments. TLC analyses were performed on silica gel plates and column chromatography was conducted over silica gel (mesh 100-200), both of which were obtained from the Qingdao Ocean Chemicals.

^{1}H-NMR and ^{13}C-NMR spectra were recorded on a Varian INOVA-400 spectrometer operating at 400 MHz and 100 MHz respectively. In NMR, the chemical shift (δ) is the corresponding resonances signal that was recorded in ppm with tetramethylsilane (TMS) as reference. The chemical shift mutiplicities were given in following format: singlet (s),

doublet (d), triplet (t), multiplet (m), double doublet (dd). Mass spectra were recorded on an LXQ Spectrometer (Thermo Scientific) operating on ESI. HRMS was recorded on a SolanX 70 FT-MS spectrometer. Absorption spectra were obtained on a SHIMADZU UV-2600 spectrometer. Fluorescence emission spectra were measured on a Thermo Scientific Lumina fluorescence spectrophotometer with 10 nm excitation and emission slit widths. The pH measurements were performed with a Swiss Mettler Toledo Five Easy Plus FE28 pH meter. Fluorescence imaging experiments were performed on an inverted fluorescence microscopy (Carl Zeiss Microscopy GmbH 37081 Gottingen, GERMANY) and a stereofluorescence microscope (SZX2-ILLT, Olympus Corporation, JAPAN). HeLa and macrophage cells (RAW264.7) were cultured in a 5% CO_2 / 95% air incubator (Sanyo, MCO-18AICUVL-PC, JAPAN). Zebrafish were incubated in illumination incubator (MGC-450BP-2, CHINA) at 28.5 °C. The cytotoxicity of the probe was measured on a Synergy|H5 microplate reader.

2.2. *Synthetic procedure*

The synthetic routes were outlined in Scheme S1.

2.2.1 Synthesis of compound 3 (coumarin 343)

A mixture of compound **4** (1.12 g, 5.18 mmol), Meldrum's acid (0.74 g, 5.18 mmol), piperidine (0.044 g, 0.52 mmol), and acetic acid (two drops) in 8 mL of ethanol was stirred at room temperature for 30 minutes. Then the reaction mixture heated to reflux for 3 hours. After cooling to room temperature, 100 mL of ice water was added in the mixture. The resulting precipitate was washed with ethanol, dried and purified by column chromatography on silica gel (CH_2Cl_2 : CH_3OH : CH_3COOH = 50 : 1: 0.1) to afford yellow product **3** (0.93 g, yield 63%). ^{1}H NMR (400 MHz, $CDCl_3$) δ (ppm): 12.497 (s,

1H), 8.506 (s, 1H), 7.022 (s, 1H), 3.412 (q, *J* = 4.8 Hz, 4H), 2.903 (t, *J* = 6.4 Hz, 2H), 2.806 (t, *J* = 6.2 Hz, 2H), 2.013 (t, *J* = 5.6 Hz, 4H); ^{13}C NMR (100 MHz, DMSO-d_6) δ (ppm): 165.074,161.081, 153.103, 149.621, 149.178, 127.940, 120.005, 107.714, 105.438, 105.182, 50.113, 49.580, 27.209, 20.920, 19.954. HRMS: m/z: calcd for $C_{16}H_{16}NO_4$: 286.10793 $[M+H]^+$, Found: 286.10775.

2.2.2 Synthesis of compound 2

Oxalyl chloride (0.6 mL, 7.1 mmol) and DMF (cat.) were added to a solution of compound **3** (100 mg, 0.35 mmol) in dried CH_2Cl_2 (10 mL). The resulting solution was stirred at room temperature for 24 hours. After the solvent being removed under reduced pressure, the obtained residue was dried under high vacuum for 2-3 hours and used directly for next step.

2.2.3. Synthesis of compound LH-1

Compound **2** was dissolved in dried CH_2Cl_2 (7 mL) and treated with a solution of the 2, 4-dinitrophenylhydrazine (70 mg, 0.35 mmol) in dried CH_2Cl_2 (5 mL) and triethylamine (1 mL, 7.2 mmol). The solution was stirred at room temperature for 48 hours. After the solvent removed under reduced pressure, the residue was purified by column chromatography on silica gel (CH_2Cl_2). The product was isolated as a yellow powder (84 mg, yield 51.6 %). ^{1}H NMR (400 MHz, $CDCl_3$) δ (ppm): 10.721 (s, 1H), 9.725 (s, 1H), 9.163 (d, *J* = 2.4 Hz, 1H), 8.594 (s, 1H), 8.297 (dd, J_1 = 9.2Hz, J_2=2.4Hz, 1H), 7.057 (s, 1H), 5.322 (s, 1H), 3.412 (m, 4H), 2.931 (t, *J* = 6.4 Hz, 2H), 2.811 (t, *J* = 6 Hz, 2H), 2.026 (m, 4H); ^{13}C NMR (100 MHz, $CDCl_3$) δ (ppm): 163.725,163.046, 153.131, 149.397, 149.298, 148.754, 130.960, 130.199, 127.552, 123.602, 120.382, 114.937, 108.282, 105.780, 105.677, 53.434, 50.438, 50.006, 27.435, 20.960, 20.013; MS (ESI):

m/z: calcd for $C_{22}H_{20}N_5O_7$: 466.14 $[M+H]^+$, $C_{22}H_{19}N_5O_7$ Na 488.12 $[M+Na]^+$. Found: 466.34 and 488.41, respectively.

2.2.4 Synthesis of compound LH-2

The synthesis procedure is similar as compound **LH-1**, and the crude product was purified by column chromatography on silica gel (CH_2Cl_2 : EtOAc = 1 : 7). The product was isolated as a yellow powder (66 mg, yield 50.4 %). ^{1}H NMR (400 MHz,$CDCl_3$) δ (ppm): 10.396 (s, 1H), 8.592(s, 1H), 7.249 (q, *J* =7.6 Hz, 2H), 7.022 (s, 1H), 6.956 (d, *J* = 7.6 Hz , 2H), 6.907(t, *J* = 7.4 Hz,1H), 5.072(br, 1H), 3.369 (m, 4H), 2.925 (t, *J* = 6.4 Hz, 2H), 2.790 (t, *J* = 6.2 Hz, 2H), 2.004 (m, 4H); ^{13}C NMR (100 MHz, $CDCl_3$) δ (ppm): 163.79, 162.70, 152.81, 148.57, 148.30, 129.11, 127.18, 121.01, 119.85, 113.86, 108.21, 107.46, 105.72, 50.29, 49.88, 27.45, 21.08, 20.15, 20.08. HRMS: m/z: calcd for $C_{16}H_{16}NO_4$: 376.16612 $[M+H]^+$, Found: 376.16579.

2.3. Determination of ClO^- in Water Sample

The crude water samples from the Yu Dai River, Jing Lake and tap water in Jiangsu University were passed through a microfiltration membrane before use. Aliquots of the water samples were then spiked with different concentrations of ClO^- (0, 5, 10, 20 μM). The results were reported as the mean ± standard deviation of triplicate experiments.

2.4. Cytotoxicity Study

RAW 264.7 cells or HeLa cells were seeded in each well of 96-well plates at a density of 1×10^5 cells/well and incubated for 24 h for cell attachment. The stock solution of **LH-1** dissolved in DMF (10 mM) was diluted with a cell culture medium containing 10% fetal bovine serum (FBS) to have a final concentration of 0, 10, 20, 30, 40 and 50 μM. Existing culture medium was replaced with 100 μL of the fresh one containing **LH-1**, and

the cells were incubated for 12 h. Then 20 μL of MTT (3-(4,5-dimethylthiazol-2-yl)-2,5-diphenyltetrazolium bromide) solution (5 mg mL^{-1}, HEPES) was added to each well. After 4 h in 37 ^{o}C, the remaining MTT solution was removed, 100 μL dimethyl sulfoxide (DMSO) was added to each well to dissolve the formazan crystals. Absorbance was measured at 490 nm on a Synergy|H5 microplate reader.

2.5. Image of exogenous ClO^- in HeLa cells

HeLa cells were cultured in DMEM supplemented with 10% FBS and 1% antibiotics (penicillin/streptomycin, 100 U/mL) at 37 °C in a 5% CO_2 / 95% air incubator. The cells were seeded on 24-well plates in the culture medium (4×10^4 cells mL^{-1}) and incubated at the incubator for 24h. Firstly, HeLa cells were incubated with 10 μM **LH-1** or **LH-2** in culture media for 30 min at 37 °C, and washed with PBS three times. Then, HeLa cells in another five groups were pretreated with 10 μM **LH-1** in culture media for 30 min, washed by PBS buffer three times, and subsequently incubated with different concentrations of ClO^- (0, 5, 10, 15, 30 μM) for another 30 min at 37 °C, and washed with PBS three times, respectively. All of the cells above were imaged by inverted fluorescence microscopy with a 20× objective lens.

2.6. Image of endogenous ClO^- in RAW264.7 cells

RAW264.7 cells were cultured in DMEM supplemented with 10% FBS and 1% antibiotics (penicillin/streptomycin, 100 U/mL) at 37 ^{o}C in a 5% CO_2 / 95% air incubator. The cells were seeded on 24-well plates in the culture medium (6×10^4 cells mL^{-1}) and incubated at the incubator for 24h. The cell experiments for imaging of endogenous ClO^- can be divided into three groups. The first group is that RAW 264.7 macrophage cells

were incubated with 10 μM **LH-1** for 30 min. In the second group, RAW 264.7 macrophage cells were incubated with 4-aminobenzoic acid hydrazide (ABAH, 200 μM) for 30 min and then incubated with 10 μM **LH-1** for 30 min. In the third group, RAW 264.7 macrophage cells were stimulated with Lipopolysaccharide (LPS, 20 μg/mL) for 12 h and then incubated with 10 μM **LH-1** for 30 min. All of the cells above were washed by PBS buffer three times before imaging and imaged by inverted fluorescence microscopy with a 20× objective lens.

2.7. Image of exogenous ClO^- in zebrafish

The 3-day-old zebrafish were incubated with **LH-1** (10 μM) for 30 min in illumination incubator, and then washed with zebrafish embryo culture water (0.1% NaCl, 0.003% KCl, 0.004% $CaCl_2 \cdot H_2O$, 0.008% $MgSO_4$) to remove the remaining probe and imaged by stereofluorescence microscope. Meanwhile, the zebrafish of other two groups were incubated with **LH-1** (10 μM) for 30 minutes followed by ClO^- (5 or 10 μM) for 30 min, and washed with culture water. Then the fluorescence imaging of zebrafish was carried out. All the experiments were strictly performed according to ethics guidelines of Regulations for the Administration of Affairs Concerning Experimental Animals published by the Bureau of Legislative Affairs of the State Council of the People's Republic of China.

3. Results and discussion

3.1 Synthesis and fluorescence properties

Probe **LH-1** was readily prepared by condensation of coumarin **343** with 2,4-dinitrophenylhydrazine. The control compound **LH-2** was also synthesized in a

similar procedure. Compared with **LH-1**, two nitro groups were absent in the molecular structure of **LH-2** (Scheme 1). All the compounds were well characterized by ^{1}H NMR spectra, ^{13}C NMR spectra and Ms spectrum. To test whether the fluorescence of coumarin 6H in **LH-1** can be completely suppressed by the two combined fluorescence quenching groups, the optical properties of **LH-1** and **LH-2** were investigated in 10 mM potassium phosphate buffer (pH 7.4, containing 20% CH_3CN as co-solvent). As shown in Figure 1, the fluorescence of both **LH-1** (Φ_f=0.0024) and **LH-2** (Φ_f=0.052) was significantly suppressed. Apparently, the fluorescence of coumarin 6H fluorophore in **LH-1** and **LH-2** could be quenched by the rotation of N-N bond. In addition, compared with that of **LH-2,** almost no residual background fluorescence was observed in **LH-1** (Figure 1 inset). This was apparently attributed to the additional d-PET process from the excited coumarin 6H fluorophore to the electron deficient 2,4-dinitrobenzene moiety in **LH-1**. To verify this d-PET process, time-dependent density functional theory (TD-DFT) calculations at the B3LYP/6-31G* level was carried out. As seen in Figure 2, the electron in the excited coumarin 6H moiety was able to transfer to the LUMO of 2,4-dinitrobenzene moiety. Thus, the d-PET process can be proceeded in **LH-1**. In contrast, no d-PET was occurred in compound **LH-2** (Figure S1). Thus, the d-PET process in **LH-1** indeed could further suppress the background fluorescence from coumarin 6H. The background fluorescence of **LH-1** and **LH-2** in a solution with different viscosity was also examined (Figure 3). Clearly, **LH-2** showed noticeable fluorescence enhancement with the solution viscosity increased, suggesting that the free rotation of N-N bond in **LH-2** was

progressively inhibited. Nonetheless, no perceptible variation of background fluorescence was observed for **LH-1** when the solution viscosity was increased. This is probably due to the high viscosity gives negligible effect on the d-PET process in **LH-1**, albeit the free rotation of N-N bond in **LH-1** was also inhibited. Therefore, by the combined effect of two fluorescence quenching groups, **LH-1** displayed extremely low residual background fluorescence, even in a solution with high viscosity, in good agreement with our design.

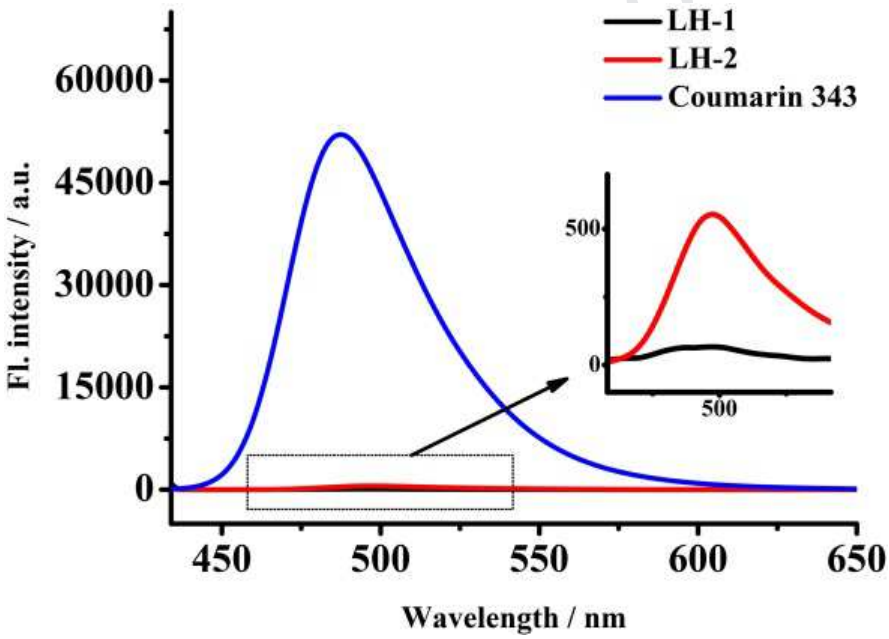

Figure 1. The fluorescence spectra of **LH-1** and **LH-2** in 10 mM potassium phosphate buffer (pH 7.4, containing 20% CH_3CN as co-solvent). For comparison, the fluorescence spectra of coumarin 343 was also displayed.

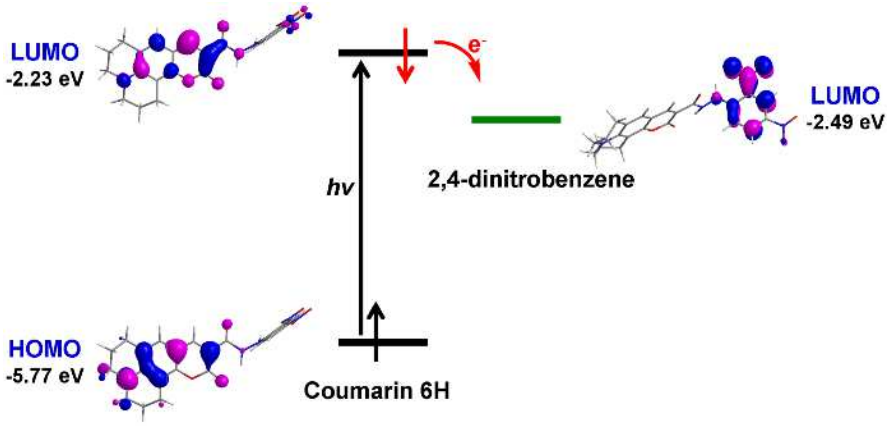

Figure 2. Frontier molecular orbital energy illustrations show the relative energetic dispositions of the orbitals of probe **LH-1**.

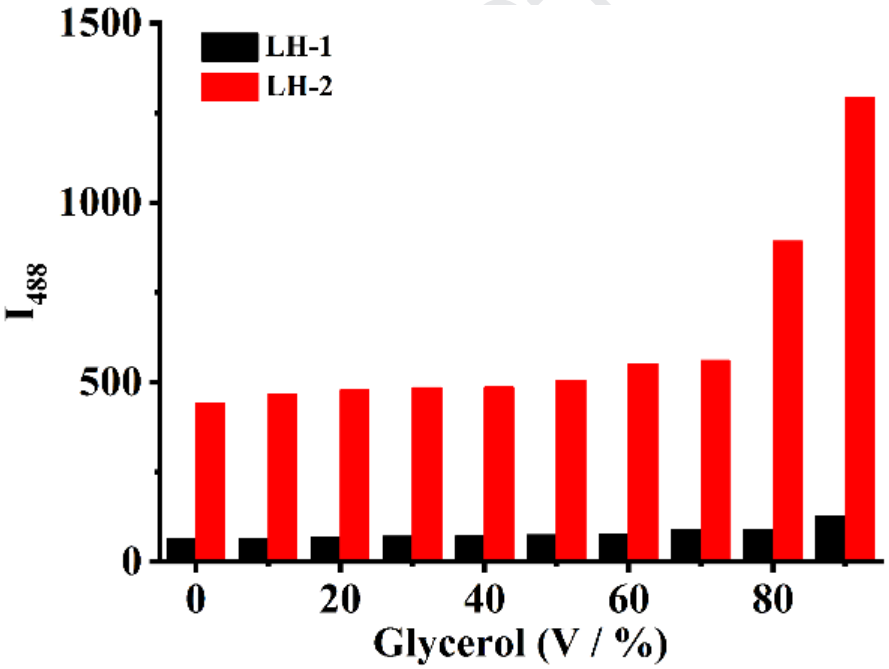

Figure 3. Fluorescence intensity at 488 nm of **LH-1** and **LH-2** (10 μM) in glycerol / acetonitrile solution as a function of increasing viscosity (λ_{ex} = 415 nm).

3.2 Optical response of LH-1 to ClO^-

The optical response of **LH-1** to ClO^- was then inspected. As design, probe **LH-1** itself

displayed no observable background fluorescence (Figure 4a). However, with the addition of increasing amount of ClO^-, dramatic fluorescence enhancement was detected at 488 nm ($\Phi_f = 0.55$), with the fluorescence color changed from dark to bluish green (Figure 4a, inset). Notably, when 40 μM ClO^- was introduced, the magnitude of fluorescence enhancement at 488 nm reached 739-fold. The drastic fluorescence enhancement implies that all of fluorescence quenching groups were removed upon treatment with ClO^-. In addition, the fluorescence intensity of **LH-1** at 488 nm showed linear relationship to ClO^- in the concentration range of 0 to 20 μM (Figure 4b), indicating that **LH-1** can be potentially used for quantitatively detecting ClO^-. Moreover, **LH-1** displayed very sensitive response to ClO^-, and the detection limits was estimated to be 10.5 nM, which is favourable for detecting minor variation of intracellular ClO^-. Recently reported fluorescent probes for ClO^- were summarized in Table S1. The results clearly denoted that **LH-1** showed superior fluorescence sensing properties to ClO^-.

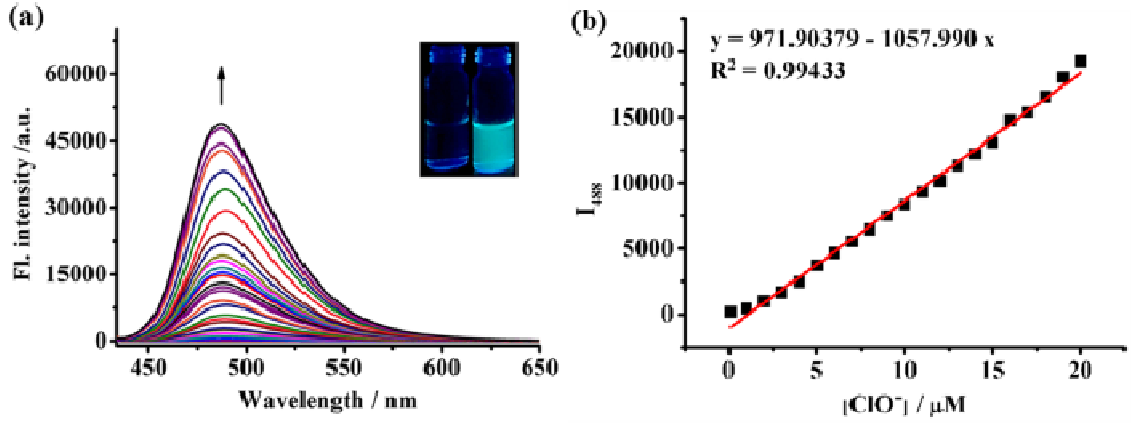

Figure 4. **(a)** Fluorescence spectra (λ_{ex} = 415 nm) of **LH-1** (10 μM) in the presence of various concentrations of **ClO^-** (0-40 μM) in 10 mM potassium phosphate buffer (pH 7.4, containing 20% CH_3CN as co-solvent). Inset: photographs of 10 μM **LH-1** without and

with **ClO$^-$** (40 μM) under a hand-hold 365 nm UV light. **(**b) The linear relationship of fluorescence intensity at 488 nm of **LH-1** (10 μM) to various amount of ClO^- (0 to 20 μM).

The UV/Vis absorption spectra of **LH-1** also showed a significant response to ClO^- (Figure S2). In the absence of ClO^-, **LH-1** displayed an intense absorption centered at 459 nm. After addition of ClO^-, the absorption was blue-shifted to 424 nm. The blue-shifted absorption suggested that the electron withdrawing fluorescence quenching groups were removed. To investigate the sensing reaction mechanism, the sensing reaction product was isolated and used for characterization. According to the high-resolution mass spectrometry (HRMS) (Figure S3), ^{1}H NMR (Figure S4), absorption spectra (Figure S5), and fluorescence emission spectra (Figure S6), the reaction product was unambiguously proved to be coumarin 343 (Scheme 1b), consistent with the sensing reaction mechanism of previous work [19].

The selectivity of **LH-1** toward ClO^- were evaluated. As displayed in Figure 5, addition of 40 μM other potential interfering species including H_2O_2, •OH, $^1O_2$, and NO caused no visible enhancement of fluorescent intensity at 488 nm. A prominent fluorescence enhancement was only triggered after the addition of 40 μM ClO^-. Furthermore, the visual fluorescence response of **LH-1** to various species (Figure 5, inset) showed that probe **LH-1** can be served as "naked-eye'' indicator for ClO^-. Also, the time-dependent fluorescence intensity changes of **LH-1** (10 μM) upon introducing different concentration of ClO^- (0, 10, 20, 30, 40 μM) were monitored (Figure 6). The fluorescence intensities at 488 nm of **LH-1** can level out after incubation with ClO^- for 20 minutes. Thus, probe **LH-1** can be employed for rapid detection of ClO^-. The fluorescence responses of **LH-1**

to ClO^- in solution with different CH_3CN volume fraction were also studied (Figure S7). Probe **LH-1** itself exhibit no background fluorescence in solution with various CH_3CN volume fraction. After addition of ClO^-, the largest fluorescence intensity enhancement was observed in a solution with 20% CH_3CN. Thereby, all the experiments for the optical response of **LH-1** to ClO^- were carried out in 10 mM potassium phosphate buffer containing 20% CH_3CN.

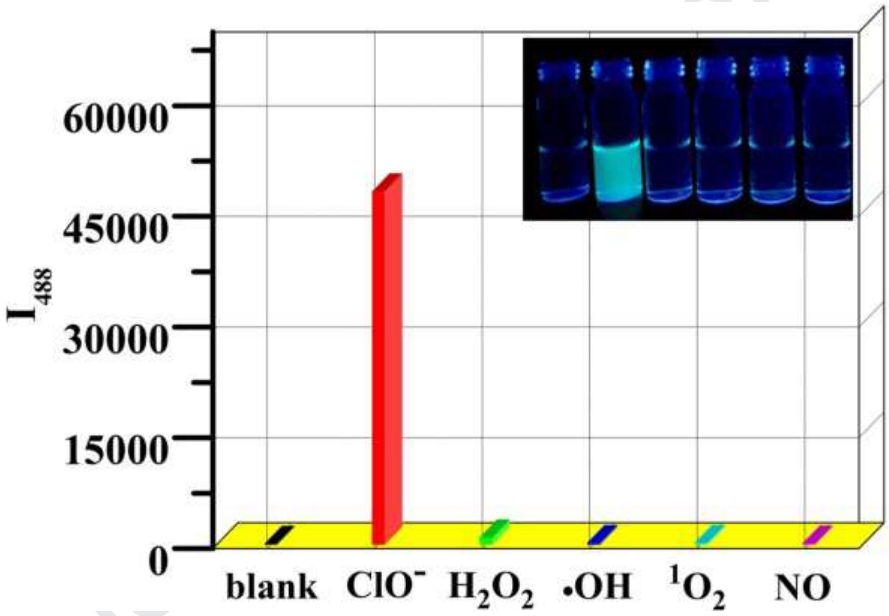

Figure 5. Fluorescence intensity responses (λ_{ex}=415 nm, λ_{em}= 488 nm) of **LH-1** (10 μM) in the presence of 40 μM various species in 10 mM potassium phosphate buffer (pH 7.4, containing 20% CH_3CN as co-solvent). Inset: visual fluorescence color changes of **LH-1** (10 μM) in the presence of 40 μM various species (from left to right: Blank, ClO^-, H_2O_2, •OH, $^1O_2$, NO).

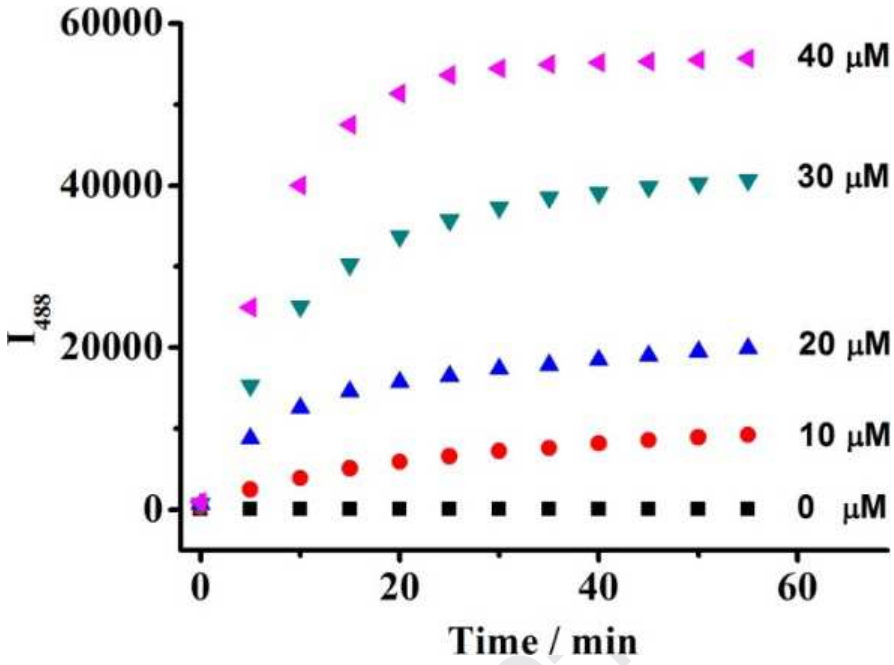

Figure 6. Time-dependent fluorescence intensity of **LH-1** (10 μM) after incubating with various concentration (0, 10, 20, 30, 40 μM) of **ClO$^-$** in 10 mM potassium phosphate buffer (pH 7.4, containing 20% CH_3CN as co-solvent) at room temperature (λ_{ex}=415 nm, λ_{em}=488 nm).

Moreover, the effect of pH value on the fluorescence response of **LH-1** to ClO^- was determined (Figure S8). In the absence of ClO^-, almost no background fluorescence was observed in **LH-1** solution in a wide pH range of 2-11. Thus, the pH value of the solution showed an ignorable effect on the background fluorescence in **LH-1**, probably because of the combined effect of two types of fluorescence quenching groups. Upon introducing 40 μM ClO^-, remarkable fluorescence enhancement was observed when the pH value of the solution was above 6.0. Consequently, **LH-1** could be used to detect ClO^- under physiological pH conditions.

3.3 Determination of ClO^- in water samples

ClO^- was widely used in our daily life, and the high-level residue of ClO^- in water may lead to hazard to human health. Thus, probe **LH-1** was applied for determining ClO^- in various water samples by means of standard addition method. The water samples were obtained from Yu Dai river, Jing Lake and tap water. No significant fluorescence enhancement was observed when **LH-1** was directly treated with the water samples (Table S2). When different concentrations of ClO^- (5, 10 and 20 μM) were added to the water samples, probe **LH-1** could detect ClO^- in these water samples with good recovery. These data led us to conclude that **LH-1** can accurately quantify ClO^- levels in various water samples.

3.4 Fluorescence imaging of exogenous and endogenous ClO^- in living cells

Inspired by the good performance of **LH-1** to ClO^- in aqueous solution, probe **LH-1** was further utilized for detecting exogenous and endogenous ClO^- in living cells. Firstly, the background fluorescence in living cells was investigated. Obviously, probe **LH-1** showed no discernible background fluorescence in HeLa cells (Figure 7a). Thus, **LH-1** can be used as a reliable fluorescent probe for detecting ClO^- in living cells. By contrast, the control compound **LH-2** still displayed weak background fluorescence (Figure 7b), probably because the relative high viscosity in living cells inhibits the free rotation of N-N group in **LH-2**.

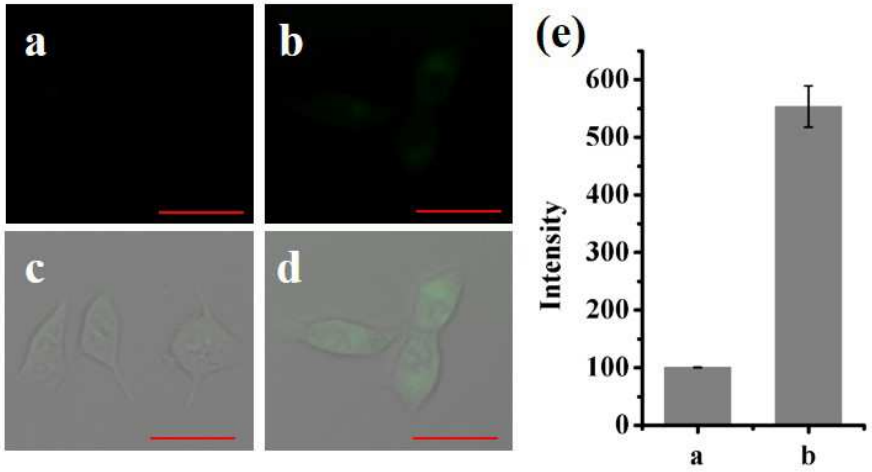

Figure 7. (a, b) The fluorescence image of **LH-1** and **LH-2** in HeLa cells, respectively; (c, d) merged image of (a) and (b) with their corresponding bright field images, respectively; (e) quantification of mean fluorescence intensity in (a) and (b) correspondingly. Scale bar: 20 μm.

Then, the fluorescence imaging of **LH-1** to exogenous ClO^- in HeLa cells was carried out. The cells were pre-stained with **LH-1** (10 μM), and then incubated with different concentration of ClO^- (0 μM, 5 μM, 10 μM, 15 μM, and 30 μM). As shown in Figure 8, the fluorescence intensities of the cells were gradually enhanced with the addition of increasing amount of ClO^-. The results indicated that probe **LH-1** had the capability to sense different concentration of exogenous ClO^- in living cells.

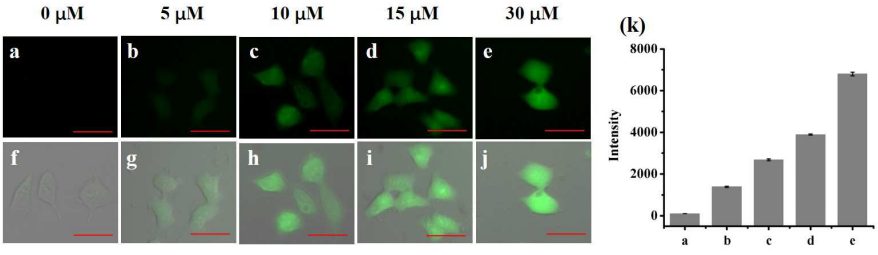

Figure 8. Fluorescence images for ClO^- detection in HeLa cells using probe **LH-1**. (a-e)

image of HeLa cells incubated with **LH-1** (10 μM) for 30 min, and then treating with 0, 5, 10, 15, and 30 μM ClO^-, respectively. (f-j) merged image of (a-e) with their corresponding bright field image. (k) quantification of mean fluorescence intensity in (a-e) correspondingly. Scale bar: 20 μm.

As probe **LH-1** displayed extremely low background fluorescence as well as highly sensitive response to ClO^-, we anticipated that **LH-1** could be applied for imaging very trace amount of endogenous ClO^- in living cells. Thus, the feasibility of **LH-1** for imaging endogenous ClO^- was investigated in RAW 264.7 cells. After incubating with **LH-1** for 30 min, the RAW 264.7 cells showed weak intracellular fluorescence (Figure 9a). However, when the cells were pre-treated with 4-amino-benzoicacid hydrazide (ABAH) (well-known MPO inhibitors [26]) for 30 min, and then further incubated with **LH-1** for 30 min, no fluorescence was observed (Figure 9b). Thus, the weak fluorescence in Figure 9a was apparently originated from basal endogenous ClO^-. Accordingly, **LH-1** was sensitive enough to detect the basal endogenous ClO^-. It is known that RAW264.7 cells may produce more concentration of endogenous ClO^- by lipopolysaccharide (LPS) stimulation [27]. Subsequently, RAW 264.7 cells were incubated with LPS (20 μg/mL) for 12 h, and then stained with **LH-1** for 30 min. Notable fluorescence enhancement was observed (Figure 9c). Therefore, probe **LH-1** was able to detect the minor variation of endogenous ClO^- in living RAW 264.7 cells. The cytotoxicity of **LH-1** was studied by MTT assays. The results demonstrated that probe **LH-1** showed low cellular cytotoxicity (Figure S9).

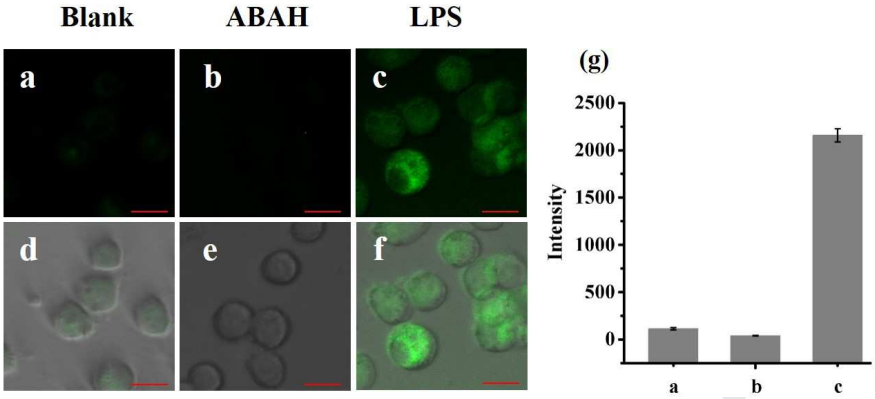

Figure 9. Fluorescence images for detection of endogeous ClO^- in RAW 264.7 cells using **LH-1**. (a) RAW 264.7 cells were incubated with **LH-1** (10 μM) for 30 min; (b) RAW 264.7 cells were pre-treated with ABAH (200 μM) for 30 min, and then incubated with **LH-1** (10 μM) for 30 min; (c) RAW 264.7 cells were stimulated with LPS (20 μg/mL) for 12 h and then incubated with **LH-1** for 30 min. (d-f) merged image of a-c with their corresponding bright field image. (g) Quantification of mean fluorescence intensity in (a-c) correspondingly. Scale bar: 20 μm.

3.5 Fluorescence imaging of ClO^- in zebrafish

Encouraged by the successful fluorescence imaging in living cells, we further explored the ability of **LH-1** for detection of ClO^- in vivo. In the control group, the 3-day-old zebrafish was stained with 10 μM **LH-1** for 30 min. Almost no fluorescence can be seen in the zebrafish (Figure 10b). However, when the **LH-1** stained zebrafish was further incubated with ClO^- (5 μM) for 30 min, a weak green fluorescence was observed (Figure 10d). Moreover, the green fluorescence become stronger after the **LH-1** stained zebrafish incubated with 10 μM ClO^- for 30 min (Figure 10f). Therefore, probe **LH-1** has the potential capacity to monitor ClO^- in vivo.

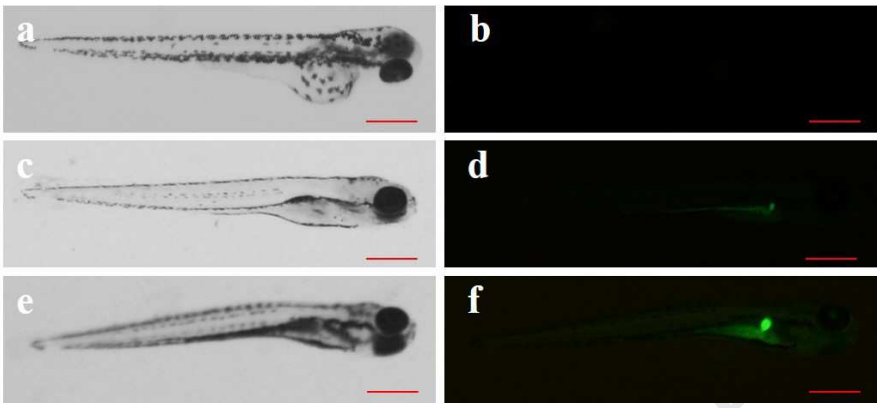

Figure 10. Fluorescence imaging of ClO^- in zebrafish: (a–b) the zebrafish was stained with **LH-1** (10 μM) for 30 min; (c–d) the zebrafish was stained with **LH-1** (10 μM) for 30 min, and then incubated with ClO^- (5 μM) for 30 min; (e–f) the zebrafish stained with **LH-1** (10 μM) for 30 min, and then incubated with ClO^- (10 μM) for 30 min; (a, c, e) the bright-fields; (b, d, f) the green fluorescence channels. Scale bar: 500 μm.

4. Conclusions

In summary, we have rationally developed a novel fluorescent probe, **LH-1**, for detection of ClO^- in water samples and biological samples. In probe **LH-1**, the fluorescence of coumarin 6H fluorophore not only can be quenched by the rotation of N-N group, but also can be quenched by the 2,4-dinitrobenzenze group via d-PET mechanism. Thus, probe **LH-1** displayed extremely low background fluorescence. Moreover, by the combined effect of two fluorescence quenching groups, the probe exhibited low background fluorescence even in a solution with high viscosity. The optical experiments indicated that probe **LH-1** displayed dramatical fluorescence enhancement response to ClO^- with high sensitivity and selectivity, and the detection limits were determined to be 10.5 nM. In addition, the

fluorescence enhancement showed good linear relationship to ClO^- in the concentration range of 0 to 20 μM. Probe **LH-1** has been applied for quantitatively detecting ClO^- in various water samples. Importantly, the fluorescence imaging experiments demonstrated that **LH-1** was successfully used for imaging the minor variation of ClO^- in living cells and zebrafish. The probe illustrated herein will be widely employed to reliably monitor the variation of ClO^- in living system.

Conflicts of interest

There are no conflicts to declare.

Acknowledgements

This work was supported by the National Natural Science Foundation of China (Grants 201105038, 51878317, 21874059), the Priority Academic Program Development of Jiangsu Higher Education Institutions, and the Jiangsu Collaborative Innovation Center of Technology and Material of Water Treatment.

References

[1] W.A. Rutala, D.J. Weber, Uses of inorganic hypochlorite (bleach) in health-care facilities, Clin. Microbiol. Rev. 10 (1997) 597-610.

[2] K.-C. Huang, C.-C. Yang, K.-T. Lee, C.-T. Chien, Reduced hemodialysis-induced oxidative stress in end-stage renal disease patients by electrolyzed reduced water, Kidney Int. 64 (2003) 704-714.

[3] S. Hammerschmidt, N. Büchler, H. Wahn, Tissue Lipid Peroxidation and Reduced Glutathione Depletion in Hypochlorite-Induced Lung Injury, Chest 121 (2002) 573-581.

[4] S.M. Wu, S.V. Pizzo, α2-Macroglobulin from Rheumatoid Arthritis Synovial Fluid: Functional Analysis Defines a Role for Oxidation in Inflammation, Arch. Biochem. Biophys. 391 (2001) 119-126.

[5] K.L. Brown, C. Darris, K.L. Rose, O.A. Sanchez, H. Madu, J. Avance, N. Brooks, M.-Z. Zhang, A. Fogo, R. Harris, B.G. Hudson, P. Voziyan, Hypohalous acids contribute to renal extracellular matrix damage in experimental diabetes, Diabetes 64 (2015) 2242-2253.

[6] N.O. Soto, B. Horstkotte, J.G. March, P.L.L.d. Alba, L.L. Martínez, V.C. Martín, An environmental friendly method for the automatic determination of hypochlorite in commercial products using multisyringe flow injection analysis, Anal. Chim. Acta 611 (2008) 182-186.

[7] J. Zhang, X. Wang, X. Yang, Colorimetric determination of hypochlorite with unmodified gold nanoparticles through the oxidation of a stabilizer thiol compound, Analyst 137 (2012) 2806-2812.

[8] H. Kodamatani, H. Yamasaki, T. Sakaguchi, S. Itoh, Y. Iwaya, M. Saga, K. Saito, R. Kanzaki, T. Tomiyasu, Rapid method for monitoring N-nitrosodimethylamine in drinking water at the ng/L level without pre-concentration using high-performance liquid chromatography-chemiluminescence detection, J. Chromatogr. A 1460 (2016) 202-206.

[9] S. Thiagarajan, Z.-Y. Wu, S.-M. Chen, Amperometric determination of sodium hypochlorite at poly MnTAPP-nano Au film modified electrode, J. Electroanal. Chem. 661 (2011) 322-328.

[10] L. Long, D. Zhang, X. Li, J. Zhang, C. Zhang, L. Zhou, A fluorescence ratiometric sensor for hypochlorite based on a novel dual-fluorophore response approach, Anal. Chim. Acta 775 (2013) 100-105.

[11] S. Kenmoku, Y. Urano, H. Kojima, T. Nagano, Development of a Highly Specific Rhodamine-Based Fluorescence Probe for Hypochlorous Acid and Its Application to Real-Time Imaging of Phagocytosis, J. Am. Chem. Soc. 129 (2007) 7313-7318.

[12] Y. Koide, Y. Urano, K. Hanaoka, T. Terai, T. Nagano, Development of an Si-Rhodamine-Based Far-Red to Near-Infrared Fluorescence Probe Selective for Hypochlorous Acid and Its Applications for Biological Imaging, J. Am. Chem. Soc. 133 (2011) 5680-5682.

[13] T. Ikeno, K. Hanaoka, S. Iwaki, T. Myochin, Y. Murayama, H. Ohde, T. Komatsu, T. Ueno, T. Nagano, Y. Urano, Design and Synthesis of an Activatable Photoacoustic Probe for Hypochlorous Acid, Anal. Chem. 91 (2019) 9086-9092.

[14] K. Kumar, S. Kaur, S. Kaur, G. Bhargava, S. Kumar, P. Singh, Self-assembled nanofibers of perylene diimide for the detection of hypochlorite in water, bio-fluids and solid-state: exogenous and endogenous bioimaging of hypochlorite in cells, J. Mater. Chem. B 8 (2020) 125-135.

[15] W. Lin, L. Long, B. Chen, W. Tan, A Ratiometric Fluorescent Probe for Hypochlorite Based on a Deoximation Reaction, Chem. Eur. J. 15 (2009) 2305-2309.

[16] Z.-N. Sun, F.-Q. Liu, Y. Chen, P.K.H. Tam, D. Yang, A Highly Specific BODIPY-Based Fluorescent Probe for the Detection of Hypochlorous Acid, Org. Lett. 10 (2008) 2171-2174.

[17] Y. Zhou, J. Li, K. Chu, K. Liu, C. Yao, J. Li, Fluorescence turn-on detection of hypochlorous acid via HOCl-promoted dihydrofluorescein-ether oxidation and its application in vivow, Chem. Commun. 48 (2012) 4677-4679.

[18] X. Zhong, Q. Yang, Y. Chen, Y. Jiang, B. Wang, J. Shen, A mitochondria-targeted fluorescent probe based on coumarin–pyridine derivatives for hypochlorite imaging in living cells and zebrafish, J. Mater. Chem. B 7 (2019) 7332-7337.

[19] L. Long, Y. Wu, L. Wang, A. Gong, F. Hu, C. Zhang, A fluorescent probe for hypochlorite based on the modulation of the unique rotation of the N–N single bond in acetohydrazide, Chem. Commun. 51 (2015) 10435-10438.

[20] X. Peng, Z. Yang, J. Wang, J. Fan, Y. He, F. Song, B. Wang, S. Sun, J. Qu, J. Qi, M. Yan, Fluorescence Ratiometry and Fluorescence Lifetime Imaging: Using a Single Molecular Sensor for Dual Mode Imaging of Cellular Viscosity, J. Am. Chem. Soc. 133 (2011) 6626-6635.

[21] S.-J. Li, Y.-F. Li, H.-W. Liu, D.-Y. Zhou, W.-L. Jiang, J. Ou-Yang, C.-Y. Li, A Dual-Response Fluorescent Probe for the Detection of Viscosity and H2S and Its Application in Studying Their Cross-Talk Influence in Mitochondria, Anal. Chem. 90 (2018) 9418-9425.

[22] Q. Sun, S.-H. Yang, L. Wu, W.-C. Yang, G.-F. Yang, A Highly Sensitive and Selective Fluorescent Probe for Thiophenol Designed via a Twist-Blockage Strategy, Anal. Chem. 88 (2016) 2266-2272.

[23] G. Yin, T. Niu, T. Yu, Y. Gan, X. Sun, P. Yin, H. Chen, Y. Zhang, H. Li, S. Yao, Simultaneous Visualization of Endogenous Homocysteine, Cysteine, Glutathione, and

their Transformation through Different Fluorescence Channels, Angew. Chem. Int. Ed. 58 (2019) 4557-4561.

[24] Y. Li, T.-S. Chu, DFT/TDDFT Study on the Sensing Mechanism of a Fluorescent Probe for Hydrogen Sulfide: Excited State Intramolecular Proton Transfer Coupled Twisted Intramolecular Charge Transfer, J. Phy. Chem. A 121 (2017) 5245-5256.

[25] J. Van Gompel, G.B. Schuster, Chemiluminescence of organic peroxides: intramolecular electron-exchange luminescence from a secondary perester, J. Org. Chem. 52 (1987) 1465-1468.

[26] A.J. Kettle, C.A. Gedye, C.C. Winterbourn, Mechanism of inactivation of myeloperoxidase by 4-aminobenzoic acid hydrazide, Biochem. J. 321 (Pt 2) (1997) 503-508.

[27] G. Li, D. Zhu, Q. Liu, L. Xue, H. Jiang, A Strategy for Highly Selective Detection and Imaging of Hypochlorite Using Selenoxide Elimination, Org. Lett. 15 (2013) 2002-2005.

Highlights

- The fluorescent probe displayed extremely low background fluorescence by a novel doubly-quenching strategy.
- The fluorescent probe showed highly sensitive and selective response to hypochlorite even with no perturbation by viscosity.
- The fluorescent probe has been applied for fluorescence imaging of exogenous and endogenous hypochlorite in living cells and zebrafish.

Author Contributions – CrediT

Zhixiang Han: Writing - original draft, Project administration, Funding acquisition, Supervision. **Lianghuan Dong**: Conceptualization, Methodology, Writing – original draft. **Fan Sun**: Software, Visualization, Writing - original draft. **Lingliang Long**: Writing - original draft, Project administration, Funding acquisition, Supervision. **Shu Jiang**: Data curation, Writing - original draft, Writing - review & editing. **Xiaoting Dai**: Writing – original draft, Methodology. **Min Zhang**: Data curation, Writing - original draft, Writing - review & editing.